Food Packaging and Shelf Life xxx (xxxx) 101226

Contents lists available at ScienceDirect

Food Packaging and Shelf Life

journal homepage: www.elsevier.com/locate/fpsl

Preparation and performance evaluation of 3D printed Poly Lactic Acid composites reinforced with silane functionalized walnut shell for food packaging application

Sabarinathan Palaniyappan [a, *], Narain Kumar Sivakumar [b], Mahdi Bodaghi [c], Mostafizur Rahaman [d], Saravanan Pandiaraj [e]

[a] Centre for Molecular Medicine and Diagnostics, Saveetha Dental College, Saveetha Institute of Medical and Technical Sciences, Saveetha University, Chennai, Tamil Nadu, India
[b] Centre for Additive Manufacturing, Chennai Institute of Technology, Tamil Nadu 600069, India
[c] Department of Engineering, School of Science and Technology, Nottingham Trent University, Nottingham NG11 8NS, UK
[d] Department of Chemistry, College of Science, King Saud University, P.O. Box 2455, Riyadh 11451, Saudi Arabia
[e] Department of Self-Development Skills, King Saud University, Riyadh 11362, Saudi Arabia

ARTICLE INFO

Keywords:
Biopolymer
Bio-composites, 3D printing
Sustainability
Biodegradation
Mechanical Properties
Food Packaging

ABSTRACT

The main goal of this work is to develop silane-grafted Poly Lactic Acid (PLA) bio-composites reinforced by various compositions of 0, 5, 10, and 15 wt% Walnut shell (WAL) particles and 3D printed by Fused Filament Fabrication (FFF) technique. The composite filaments are extruded by filament extrusion technique, and the 3D printed Walnut shell/PLA (WAL/PLA) bio-composite samples are evaluated for various mechanical, water absorption and biodegradation properties. The effect of silane grafting increases the crystallinity index value of 61.2% for the silane-grafted WAL particles. The mechanical property results reveal that using WAL particles reduces the strength value and improves the modulus of both untreated and silane-treated WAL/PLA composites. The silane grafted 15% WAL/PLA samples show the highest shore hardness value of 71 MPa and the heat deflection temperature of 63.79 °C. The biodegradation test results reveal that the untreated 15% WAL/PLA composites have a higher mass loss of 6.4% and 19.1% for 30 and 60 days, respectively. Fractographical results of silane-treated 10% WAL/PLA composites exhibit a uniform distribution of WAL particles with minimum particle pull-out from the polymeric matrix. The findings of this study affirm the potential of WAL/PLA bio-composites as a viable and sustainable material for application in food storage and service.

1. Introduction

Food packaging concerned with the quality and safety of the food products during the processing, such as storage, transportation and distribution (Ahmed et al., 2023). In general, plastics are the most preferred materials in various packaging applications due to their key properties such as high strength-to-weight ratio, better physical and mechanical properties, manufacturing at low melting temperature, optical and wetting properties (Dang et al., 2012). Most of the commonly used plastics in food packaging applications are Poly Lactic Acid (PLA), Poly Vinyl Chloride (PVC), Polyolefin (PO), Polyamides (PA), and Polyesters (Vroman and Tighzert, 2009). In general, plastic packaging material produces 67 million tons of waste from the sea and it generates huge environmental issues to marine ecosystem (Song et al., 2009). It leads to various environmental risks in terms of creating pollution to humankind and nature. In order to overcome these kinds of environmental problems, biodegradable polymers are considered for packaging applications (Silveira et al., 2020). It's quite challenging to eliminate conventional plastics, but it is possible to replace them with biopolymers.

Among the various biopolymers, PLA is the most commercially successful polymer due to its key properties such as easy processability and biodegradability. But the main limitation is that it possesses poor mechanical property and higher brittleness compared to other conventional polymers (Rasal et al., 2010). To boost the mechanical properties of the PLA polymers, there are various methods like blending or adding

* Corresponding author.
E-mail addresses: sabarinathan14010@mech.ssn.edu.in (S. Palaniyappan), narainkumars.mech2020@citchennai.net (N.K. Sivakumar), mahdi.bodaghi@ntu.ac.uk (M. Bodaghi), mrahaman@ksu.edu.sa (M. Rahaman), psaravanan.c@ksu.edu.sa (S. Pandiaraj).

https://doi.org/10.1016/j.fpsl.2023.101226
Received 14 July 2023; Received in revised form 29 November 2023; Accepted 11 December 2023
2214-2894/

suitable bio filler into the PLA polymeric matrix (Li et al., 2015). There are various studies that show that addition of bio fillers improves the mechanical properties such as tensile strength, thermal and wear resistant properties of the prepared polymeric composites (Du et al., 2014; Zhang et al., 2021; Palaniyappan et al., 2022). The strength of the prepared bio filler reinforced polymer composite depends on various properties such as filler size, filler distribution in polymer matrix, interfacial adhesion and morphology of the added fillers (Essabir et al., 2013; Cheang and Khor, 2003).

Natural fillers are composed of various constituents such as cellulose, wax, hemicellulose and lignin. Shell based natural fillers are rich in source of cellulose and can be considered for reinforcement in the polymer composite preparation (John and Thomas, 2008). In walnut food processing, walnut shell portion comprises of about 67% and almost 1.5 metric tons of hulls are dumped as fossil fuels every year (Hemmati et al., 2018; Demiral and Kul, 2014). Those hulls are lignocellulosic material which comprises of cellulose - 25.60, lignin - 52.30, hemicellulose - 22.10 and ash - 3.6% (Pirayesh et al., 2012). Therefore, utilization of walnut shell particle as bio fillers in polymer composite preparation could have a dual benefit of considering environmental impact of fossil fuel and effective reinforcement in composite preparation. Several studies concentrated on utilizing the walnut shell as a reinforcement for the development of bio-composites using conventional manufacturing techniques. Ayrilmis et al. added walnut shell of 40–60% as reinforcement for the production of polypropylene composite and the results show that the added bio filler increases the bending and tensile properties of the respective composites (Ayrilmis et al., 2019). Sarsari et al. assessed the mechanical properties of the wood particle reinforced polylactic acid composites using injection moulding technique. The results highlighted that up to 40% of walnut shell particle composition drastically increases the tensile strength effectively (Sarsari et al., 2016). Liu et al. developed amino functionalised walnut shell reinforced poly lactic acid composite by injection moulding technique. The observed results specifies that the produced composite is limited for the making of complex components (Liu et al., 2014). In order to improve the interface adhesion of the added reinforcement with polymeric matrix various surface modification techniques are employed.

Surface modification techniques includes physical, thermal, chemical and UV curing techniques, chemical modification technique possesses better advantages over the other surface modification techniques. Silane grafting is one of the most preferred chemical surface modification processes for preparing the two different organic and inorganic mixed composite preparation (Vishal et al., 2022). During the silane modification, the silane molecules act as a coupling agent and the bi functional features of silane on the hydroxyl group (Si-O-filler) of the filler and the other end react with the polymeric matrix (Tran et al., 2014). Zhou et al. studied to improve the UV protection and mechanical properties of PLA polymer by silane induced carbon nitride grafting. The results show that, the 1% of graphitic carbon nitride coupled with KH570 silane solution exploits the higher ductility and elongation and break (Zhou et al., 2023). Similarly, sun et al. made a study on the delayed photodegradation of the PLA composite by adding silane KH550 and KH570-treated micro-nano rice husk fibres as reinforcement. The results implies that the silane grafted fibres reinforced composites exhibits delayed photodegradation compared over the non-grafted nano rice husk fibres reinforced PLA composite (Sun et al., 2023).

In food packaging, the cost of the packing materials decides the cost of the final food products. To reduce the cost of the packaging material, the Fused Filament Fabrication (FFF) method can be opted (Mathiazhagan et al., 2023). In FFF process, the thermoplastic materials are melted and deposited layer by layer with the help of extruder setup. The most suitable materials for the FFF process are PLA, Acrylonitrile Butadiene Styrene (ABS), Polyurethane (PU), Polystyrene (PS) and Polyether ether ketone (PEEK) (Peterson, 2019). There are various research studies concentrated on the 3D printing of commercially available polymeric materials with various bio fillers as reinforcement. Veeman et al. extruded the polymeric filaments by adding almond shell particle as bio filler and studied the compression properties of the 3D printed composites. Increasing the almond shell particle percentage improves the compressive properties compared with neat PLA polymer (Veeman and Palaniyappan, 2022). Singh et al. developed the Poly Lactic Acid composite feedstock by adding different percentage of almond shell particle (0–5 wt%). The results confirm that, the almond shell of 2.5 wt% has better mechanical properties than the other type of reinforcement added composites (Singh et al., 2020a). Yurttas et al., 3D printed polylactic acid reinforced with Liquidambar orientalis leaf extract with reduced silver nano particles. The results depict, the addition of the nano particles may enhance the antibacterial property (Yurttas et al., 2023). Ahmed et al. studied the impact of graphene oxide in the PLA matrix for the development of composite films. The results show that, the addition of graphene oxide has improved the glass transition temperature and crystallization temperature of the developed composite (Ahmed et al., 2021). Yurttas et al. modified the wood flour particle and extruded the PLA polymeric filaments for 3D printing applications. The results show that, the silver nitrate treatment with 10% particle concentration imparts the maximum mechanical and thermal properties (Yurttas and Ayrilmis, 2023).

The main drawback occurred in the previous work is the untreated particles which possess the initiation of layer debonding due to the added organic particle. In order to improve the layer adhesion and particle matrix adhesion, an attempt was made with surface modification on the added organic walnut shell particle. Therefore, there is a wide variety of organic reinforcements that are used for the development of 3D printing filaments and composites. The sustainable packaging materials should be biodegradable and possess good quality in strength. In the present, there is no chemical functionalization method to improve the strength of the 3D printed composites. There are limited studies only reporting the enhancement of strength by surface functionalization of the added organic particles.

The main objective of this work is to develop a 3D printed biodegradable PLA bio-composites with various weight percentage of (0, 5, 10, 15 wt%) untreated and silane functionalized walnut shell particles. Variation occurred during the silane chemical modification on the walnut shell particles is analyzed by X-ray diffraction and Fourier Transform Infra-Red (FT-IR) Spectroscopic technique. The quality of the extruded filaments for the 3D printing process is accessed based on the physical properties and melt flow index value. Further the mechanical strength, water absorption and thermal stability of the 3D printed component are analyzed to evaluate the usage in practical applications. Fractographical analysis of the fractured samples are examined using the scanning electron microscopic technique to find out the mode of fracture. Finally, bio degradation behaviors of the developed PLA bio-composites are accessed to employ for food packaging applications.

2. Materials and Methods

2.1. Raw materials

In the present study, PLA is selected as the raw material, procured from Nature Works Co., Ltd., USA. The PLA granules are extrusion grade with a trade name of INGEO 3D850 (ρ = 1.24 g/cc; Melt flow rate = 7–9 g/10 min; Tm = 165–180 °C).

Walnut fruit hulls are offered by the local nut-dealing industries located in India. The walnut shells are cleaned from impurities and crinkled using the Willys mill. The size-reduced walnut shell particles are sieved to their respective sizes and used as reinforcement for the next stage of the filament extrusion process. Fig. 1 shows the processing of walnut shell into particles.

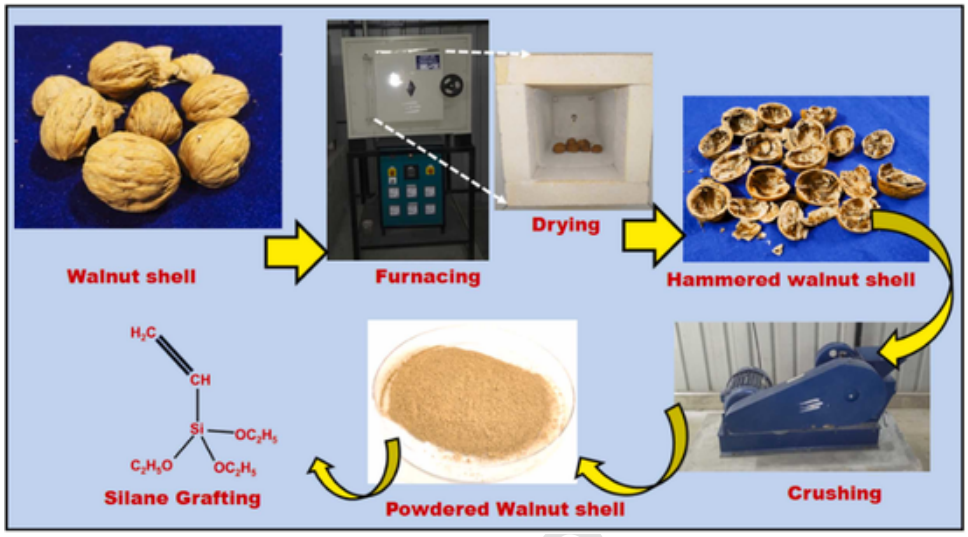

Fig. 1. Schematic procedure for generation of walnut shell particles.

2.2. Synthesis and chemical surface modification of walnut bio filler

Walnut shell (i.e., WAL) particle surfaces are processed by suitable chemical surface modification techniques to improve their adhesive properties with the polymeric components. In the current study, the silane modification technique is opted for, and the prepared WAL particles are undergone a silane treatment with a surface-modifying reagent of Tri vinyl ethoxy silane (Sigma Aldrich, UK). The silane mixture consists of 5% of silane solution in the water and ethanol with a ratio of 20:80. Further, the pH of the mixture is kept constant by adding a few drops of acetic anhydride solution. The prepared WAL particles are mixed into the solution by mechanical stirring for 15 min, filtered using Whatman filter paper and dried for 30 min at room temperature. The surface functionalized WAL particles are further dehydrated in a vacuum oven at 80 °C for 12 h. Further, the particles are used for the characterization and filament extrusion.

2.3. Characterization of surface modified walnut bio filler

X-Ray diffraction (XRD) studies of the WAL particle are conducted using the D8 Advance-Bruker X-Ray diffractometer, to analyze the crystallinity structure and index of the WAL particles. The experiment is conducted with a diffraction angle of 10–60° with an operating voltage of 40 kV. Fourier-transform infrared spectroscopy (FTIR) study analyses the functional modification occurred during the silane treatment process. In this study, Bruker alpha FTIR spectrometer is used with transmittance mode and range of 400–5000 cm^{-1} in an ATR mode. The functional group modifications such as hydroxyl, amino and other functional groups are identified by this study.

The particle morphology and size of the crushed particles are measured using the scanning electron microscopy (Make: JEOL, US). The elemental analysis of the untreated and silane treated WAL particles are identified to elaborate the oxygen to carbon ratio of the WAL bio filler.

2.4. Extrusion of silane functionalized walnut shell reinforced PLA filament

The untreated and silane functionalized WAL particles of various composition such as 0,5,10 and 15 wt% are used for the composite PLA polymeric filament extrusion. The composite WAL/PLA polymeric filaments are squeezed out by the single screw extruder. Initially the PLA polymer and the WAL particles are assorted by the compounding unit, further the mixed WAL /PLA granules are fed into the hopper of the extruder. The extruder is operated with an extrusion temperature of 155–165 °C and a speed of 200–300 rpm. Further the WAL/PLA filaments are winded automatically and the diameter is maintained of about 1.75 ± 0.06 mm for each composition. Fig. 2 shows the WAL/PLA polymeric composite filament extrusion procedure.

2.5. 3D printing of WAL/PLA polymer composites

The feedstock material for the current study is selected based on the WAL/PLA filament composition. The feedstock material is loaded in the commercially available FFF printer (Make: Pratham 3.0, India). The design models of the mechanical testing samples are considered using the design software. Further the developed models are sliced using CURA software. The developed G codes are given as an input for the model to be 3D printed. The constant printing parameters such as printing speed of 20 mm/sec, infill pattern of line, printing bed temperature of 60 °C, infill density of 100%, and layer height of 0.1 mm is considered for the FFF process of the various composition of WAL/PLA polymer composites.

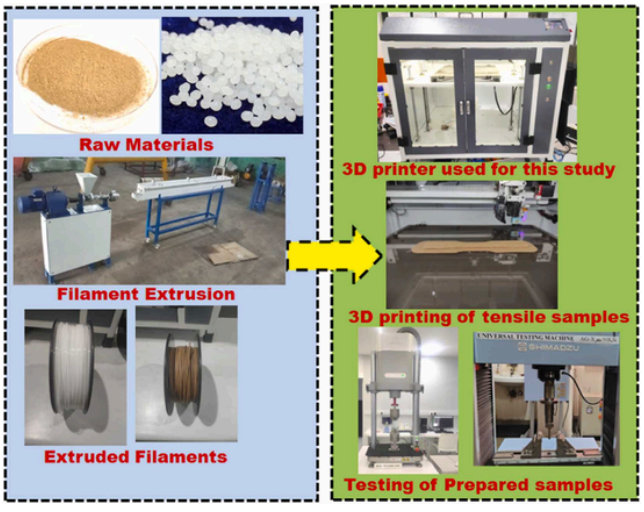

Fig. 2. Process layout for WAL/PLA filament extrusion and 3D printing.

2.6. Physical and mechanical property analysis

The density of 3D printed untreated and silane treated WAL/PLA bio polymeric composite is analyzed using the ASTM standard in a density tester. Initially the mass of the 3D printed WAL/PLA polymer composite sample in air and water is analyzed using the weighing scale. The measured mass values of each composition and density of the water are used for calculating the density of the respective composites. The density of the respective 3D printed WAL/ PLA composite is measured using the Eq. (1),

$$\rho = \frac{M_a \rho_w}{M_a - M_w} \quad (1)$$

where M_w and M_a indicate the mass of the samples in water and air, and ρ_w density of water is 1 g/cm^3.

Mechanical properties of the different composition of WAL/PLA 3D printed composite are conducted as per the ASTM standard. Tensile, flexural and compression tests are assisted in Universal Testing Machine (Make: Shimadzu, Japan) with a strain rate of 2 mm/min with various attachments. Tensile test is done as per the ASTM D638 standard and the dog bone shaped tensile test samples with a dimension of 63.50 mm × 9.53 mm × 3.4 mm is 3D printed. Flexural test is done as per the ASTM D790 standard, the experiment was done with a three-point bending set up attached with the machine. Rectangular shaped flexural samples are 3D printed with a dimension of 125 mm × 12.7 mm × 3.4 mm. Compressive test experiments are carried out as per the ASTM D695 standard for the various composition of untreated and silane treated 3D printed WAL/PLA composites. The cylindrical compression samples are prepared with a dimension of 12.7 mm × 25.4 mm and the compressive load acting on the flat faces of the sample.

Impact test of the various composition of 3D printed WAL/PLA polymer composite is assisted as per the ASTM D6110 standard via a Charpy impact test machine. The samples are 3D printed with a dimension of 126 mm × 12.7 mm × 5 mm. For considering various tensile, flexural, compression and impact tests, for each composition and test settings five samples are tried and their average values are measured and reported.

2.7. Melt flow index of the extruded filaments

The processing condition and uniform flowability of the extruded filament is measured using the melt flow index value and the test is done in a Meltfixer LT, with an extrusion load of 2.16 kg with an extrusion temperature of 180 °C. The parameters are kept constant for various compositions (0,5,10,15%) and treatment (untreated and silane) on WAL particles reinforced composites. For each test conditions, the samples are extruded for 10 times and the values are noted and the average value is finally considered for the melt flow index value of the respective WAL/PLA composites.

2.8. Water contact angle

Surface phenomenon such as capillarity mode of water absorption for the 3D printed WAL/PLA bio composites with respect to various composition percentage and surface modification is identified using the contact angle measurement technique via the Ossila contact angle goniometer (UK). The experiment is conducted by sessile drop method, in that distilled water of 5 μL is sited over the width of the 3D printed composite surface. The contact angle is calculated in both the right and left sides of each composite three times, with the average value being the mean contact angle for the respective WAL/PLA composite.

2.9. Water absorption test

Water absorption test of the 3D printed WAL/PLA composite is done to measure the swelling behavior of the composite under different environmental conditions. As per the ASTM D570–99 standard, the water absorption WAL/PLA samples are 3D printed with a dimension of 39 mm × 10 mm × 3.4 mm. The printed samples are dried, and the dry weight is measured as W_i and the WAL/PLA samples are engrossed in different types of water conditions such as normal water, hot water and sea water for 24 h. Then the WAL/PLA samples are taken out, and the excess water are wiped off and the final weight is noted as W_f. Based on the variation in the mass of the WAL/PLA sample, the swelling behavior or water absorption percentage of the composite is measured and the typical Eq. (2) for measuring the water absorption behavior of the various 3D printed WAL/PLA composite is mentioned below,

$$Water \quad Absorption \quad (\%) = \frac{W_f - W_i}{W_i} * 100 \quad (2)$$

whereas, W_i measures the initial weight of the WAL/PLA sample before water immersion and W_f represents final weight of the WAL/PLA sample after water immersion.

2.10. Biodegradability analysis

Biodegradation phenomenon of the developed WAL/PLA composite is analyzed using the soil burial test. The test is made in a closed environment, the organic soil which have the constituents of coco peat, charcoal, fine sand and microorganisms are used as the source for the experimentation. During the soil burial test, the soil moisture content is maintained at 40%, the evaporated water is adjusted by spraying the distilled water on the surface of the organic soil. During the test, 10 mm × 10 mm × 3.4 mm cross section samples are used, the WAL/PLA samples are washed with ethanol and dried in vacuum oven at 45 °C. Samples are placed inside the sand for the period of 30 days and 60 days of time interval. The sample is then cleaned and dried in the furnace. After that, the WAL/PLA polymeric sample weight is measured to estimate the biodegradation rate of the WAL/PLA composite. The biodegradation rate of the composite is measured by Eq. (3) mentioned below,

$$Mass \quad loss\,(\%) = \frac{W_b - W_a}{W_b} * 100 \quad (3)$$

in which W_b denotes the mass of the WAL/PLA sample before soil burial, and W_a represents mass of the WAL/PLA sample after soil burial.

2.11. Fractography analysis of the tested samples

Distribution of the WAL particle in the PLA matrix is measured using the Scanning Electron Microscopy technique. Tensile fractured WAL/PLA samples of different compositions are further analyzed, and the fracture morphology is examined to evaluate the mode of fracture of the respective bio-composite.

3. Results and discussion

3.1. FTIR and XRD analysis of untreated and silane functionalised WAL particles

Fig. 3(a) shows the FTIR spectra of the untreated and silane grafted WAL particles and it clearly shows the functional modification based on the peak shifting and absence of the respective functional group. The detected spectra at 3618–3009 cm^{-1} depicts that O-H stretching of H-bonded alcohol, phenol and water groups, and it is unaffected in both untreated and silane treated WAL particles. The peak present in 2915 and 2837 cm^{-1} matches to CH stretching of cellulose and hemicel-

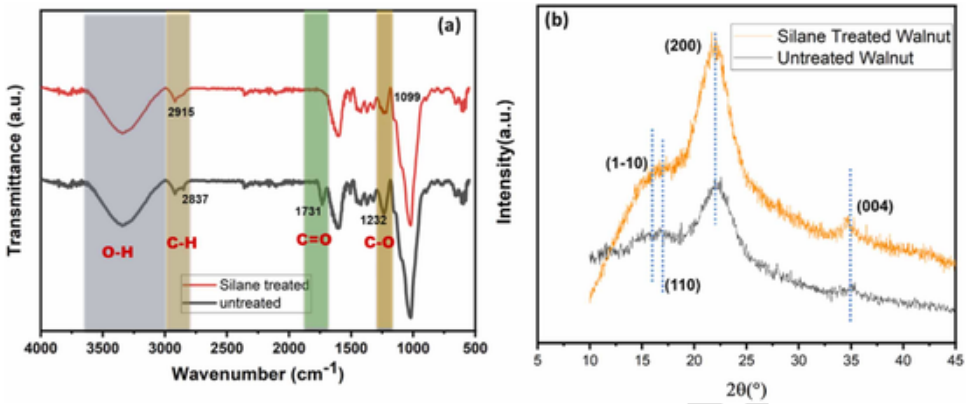

Fig. 3. (a) FTIR spectra, and (b) XRD Spectra of untreated and silane treated walnut shell particle.

lulose, those peaks are strong and intense, and they are not hydrolysed under silane grafting. For the untreated WAL particles, there is a presence of peak at 1731 cm^{-1} matches to C═O stretching of carboxylic acid and the ester group of hemicellulose. It is not appeared in the respective silane grafted WAL powders. Likewise, the peak in the range of 1232 cm^{-1} corresponds to C-O stretching of the acetyl group of hemicellulose. These peaks are present in the untreated WAL particles and the peak intensity is drastically condensed for the silane grafted WAL particles. From the observed results of peak condensed at 1232 cm^{-1}, which is an indication that removal of strength reducing substances from the organic fillers by suitable chemical modifications process. Likewise, the silane treatment has effectively removed the hemicellulose of hemp fibre in a study by Swapan et al (Sawpan et al., 2011). By considering the peak that corresponds to 1449 and 1359 cm^{-1} related to CH_2 and CH bending of cellulose it is unaffected in the silane grafted WAL particles. The peak present in 903–1158 cm^{-1} refers to C-O stretching of polysacharides in the cellulose. It results the silane treatment which does not alter the basic properties of the organic reinforcements. Finally, regarding the effect of silane grafting, there is an additional weak peak present in the range of 1099 cm^{-1} and called asymmetric stretching of Si-O-Si bond from the silane solution. Due to the condensation reaction of cellulose from the WAL particles with silane solution, the Si bond has been grafted on the cellulose structure (Hong et al., 2008).

Fig. 3(b) shows the X-Ray diffraction analysis of the untreated and silane grafted WAL particles. The major peak observed at 2° angle of 15.88°, 17.46°, 22.31°, and 35.06° with a corresponding lattice plane of (1−10), (110), (200), and (004) is an indication of cellulose I crystallites. The XRD results clearly shows that, the cellulose 1 crystalline planes of the silane grafted WAL particles which does not overlap with the untreated WAL particles. It shows the good amount of cellulose were present in the both the WAL particles. The outcome of silane treatment, the structural alteration from cellulose I to cellulose II is not arisen on the WAL particles. Manimaran et al. concluded the similar observation on the structural change of cellulose on the nendran banana peduncle plant (Manimaran et al., 2020).

$$Crystalllinity \quad Index\,(CI) = \frac{I_{Cr} - I_{am}}{I_{cr}} * 100\% \tag{4}$$

where $I_{am,}$ and I_{cr} denote amorphous intensity and crystalline intensity at an angle (2θ).

The crystallinity index of the WAL particle is considered based on the above-mentioned equation. The results show that 55.3% and 61.2% of crystallinity value is observed on the untreated and silane treated WAL particles. This result is an indication of removal of other unwanted elements such as pectin, wax, hemicellulose from the WAL particle. It results in better cellulose packing on the walnut shell with effective removal of amorphous material. A similar observation on the silane treated fish tail palm fibre has effectively removed the amorphous strength reducing substances from the fibre surface (Sabarinathan et al., 2020). It could result in improved interfacial adhesion and strength enhancement with utilization in the polymer composites.

3.2. SEM and EDX analysis of functionalised WAL particle

Fig. 4(a and c) shows the SEM images of untreated and silane treated WAL particles. SEM analysis of untreated WAL particles shows presence of surface impurities such as wax, pectin and hemicellulose on the surface of the WAL particle. And the silane grafted WAL particles in Fig. 4(c) shows the smooth surface and removal of those unwanted impurities. Further those surfaces which are containing the serrated profile displays an indication of siloxane layer coated on the walnut shell surfaces. This silane coating will improve the interlocking of polymer with the added organic particles. Similar remark on the silane grafting was made by Cai et al. on the natural fibre composites (Cai et al., 2015). Fig. 4(b and d) shows the elemental mapping of the untreated and silane treated WAL particles. From the observed outcomes, the elements present in the WAL particle are oxygen, carbon, manganese, sodium, calcium and other constituents. The reason for analysing the EDX analysis on the functionally modified walnut shell is to identify its oxygen to carbon ratio. The untreated and silane treated WAL particles reveal the oxygen to carbon ratio of 0.70 and 0.79, respectively. According to the results, the maximum oxygen to carbon ratio is detected on the silane treated WAL particle. This is due to reduction of carbon content such as impurities such as lignin, and hemicellulose from the WAL particle surface during chemical modification process. Similar report indicates the silane surface modified kigelina Africa natural fibre shows improved oxygen to carbon ratio compared with untreated natural fibres (Vishal et al., 2022).

3.3. Physical properties of the prepared 3D printed PLA/ WAL composite

Table 1 reports the various configuration and designation of 3D printed WAL/PLA composites. The physical properties of the prepared WAL/PLA composite are measured before analysing the mechanical properties. The observed density results of various untreated and silane treated WAL/PLA composites show that, adding of WAL particles decreases the density value. This is due to the WAL particle which exhibits lowest bulk density value of 0.52 gm/cc. The lowest density of 1.138 gm/cc is dictated on UN15 composite, and for considering the silane grafted composites SN15 composites shows the lowest density of 1.142 gm/cc. This is because the effect of silane treatment of the surface impurities is detached and increases the cellulose crystallites in the WAL particles. The void content or porosity is a measure of number of voids present in the prepared 3D printed samples. Maximum void content of 2.47% is dictated on UN15% composite followed by

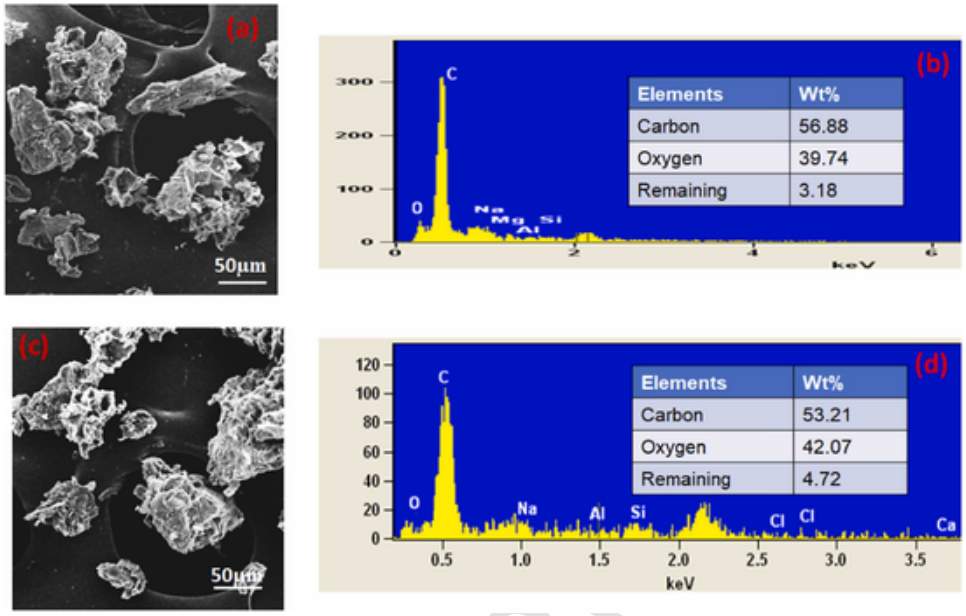

Fig. 4. SEM and EDX analysis of walnut shell (a and b) untreated and (c and d) silane treated.

Table 1
Physical properties of the developed PLA/ WAL composites.

Sl No	Sample Designation	Type of treatment	PLA (wt%)	Walnut shell (wt%)	Density (g/cm^3)	Porosity (%)
1	UN0	No treatment	100	0	1.22	1.52
2	UN5	Untreated	95	5	1.184	2.04
3	UN10	Untreated	90	10	1.154	2.27
4	UN15	Untreated	85	15	1.138	2.47
5	SN5	Silane Treated	95	5	1.210	1.195
6	SN10	Silane Treated	90	10	1.159	2.09
7	SN15	Silane Treated	85	15	1.142	2.21

SN15% composite of 2.21%. By adding or increasing in the WAL particle composition in the PLA composite, the void content is increased. This is due to added organic filler such as WAL particles which is hydrophilic in nature and with increases in WAL particle composition there is a steep rise in the void content of the composites. The 3D printed samples, deposited layer by layer, are also the reason for the increases in the porosity of the composite. The observed void content results show that the maximum void content value is less than 5% and the composites are most suitable for the commercial applications (Sreekumar et al., 2009).

3.4. Mechanical properties of the 3D printed WAL/PLA composite

3.4.1. Tensile properties

Fig. 5(a) shows the tensile strength results of the untreated and silane treated WAL/PLA polymer composites. The maximum tensile strength of 37.31 MPa is dictated on the neat 3D printed PLA composite. Addition of (WAL) particles reduce the tensile strength property with respect to neat PLA polymer. Among those untreated WAL particle reinforced PLA composites, the composites designated with UN10 composites exhibits the maximum tensile strength of 27.1 MPa followed by UN15 of 26.7 MPa and UN5 composites of 22.52 MPa. Initially the addition of reinforcement shows an increasing trend in the tensile strength, and beyond 10% there is a marginal decrease in the tensile strength value.

For the silane grafted composites, the composite with SN10 displays the highest tensile strength of 29.19 MPa. The results clearly indicate that the silane grafting of organic reinforcements enhance the tensile strength effectively. Compared with the untreated WAL/PLA composites, the silane treated WAL composites with 5,10%, and 15% composition increases the tensile strength by 6.79%, 7.7% and 2.84%. It is due

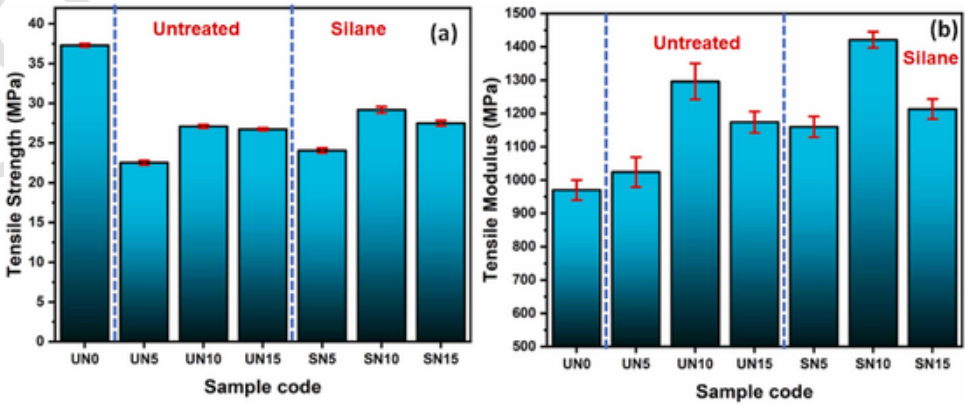

Fig. 5. (a) Tensile strength and (b) Tensile modulus of WAL/PLA composites.

to the untreated WAL composite as there is a presence of hemicellulose, lignin and wax on the walnut shell. It will increase the brittleness of the composite and the samples cannot bear higher load withstanding capability (Phuong et al., 2007). With the incorporation of silane grafted composites, the substances that weaken the strength are eliminated, leading to an enhancement in the tensile strength of the composite. The formation of a siloxane bond enhances the interfacial adhesion between the WAL fillers and the polymeric matrix in the composite. Similar results indicating improved tensile properties were observed by Luo et al. in their study on silane grafted corn fibre-reinforced PLA composites (Luo et al., 2016).

Fig. 5(b) shows the tensile modulus results of the untreated and silane treated WAL/PLA polymer composites. The maximum tensile modulus of 1421 MPa and 1296 MPa is detected on the silane treated and untreated 3D printed PLA of SN10 and UN10 composites. The lowest tensile modulus of 970 MPa is read for the neat PLA composites and is 46.41% and 33.60% lower than the silane treated and untreated 3D printed PLA of SN10 and UN10 composites. Increasing the organic WAL particles in the PLA matrix shows an increase in the tensile modulus up to 10% for both composites. It is due to the added WAL particles which share the applied load to the PLA matrix and it results in increased stiffness than the neat PLA composite. Likewise considering the silane treated reinforcements exhibits higher tensile modulus than the untreated WAL particle added composites for all the compositions. This is because of the surface modification of walnut shell by the Si–O–CH_3 functional group which enhances the interfacial adhesion of the WAL particle with the PLA polymer. The primary chain of silane remains compatible with the nonpolar PLA, thus enhancing the adhesion at the interface between the WAL filler and PLA in the two-phase system. This compatibility is achieved because the silane can undergo hydrolysis, forming silanol groups that interact with both the WAL and the PLA matrix. Liu et al. observed similar results on increased tensile modulus due to the silane modification on the added wood flour PLA composite (Liu et al., 2016).

At 15% concentration of untreated and silane treated UN15 and SN15, composites exhibit lower tensile modulus value of 1174 MPa and 1213 MPa than the 10% composites. It is due to improper interfacial adhesion of WAL particle with matrix which results in an unbalanced load sharing with the PLA polymer. The reduction in mechanical strength upon subsequent loading can be attributed to insufficient wetting of the higher concentration of added particles within the matrix. This incomplete wetting results in a higher susceptibility to composite failure. The increase in wood particle content is a result of the reduced flexibility of the matrix, which is constrained by the presence of rigid particles (Hamming et al., 2009).

3.4.2. Flexural properties

Fig. 6(a) shows the flexural strength results of the untreated and silane treated WAL/PLA polymeric composites. The maximum flexural strength of 53.25 MPa is detected on the neat 3D printed PLA composite. Increases in the WAL particle content shows a decreasing trend in the flexural strength value. The maximum flexural strength values 47.29 MPa on the untreated 5% WAL particle reinforced 3D printed composites. During the 3D printing process, the extruded filaments which consists of WAL particle and molecular chain of the PLA polymer is oriented along the X-Y plane. Under flexural loading, the load acts on the sample perpendicular to the stress direction (Z plane). The interfacial layer adhesion majorly influences in the enhancement of the flexural strength of the 3D printed polymeric composites (Liu et al., 2019). In case of silane functionalized WAL/PLA composites, they show higher flexural strength value of 49.1 MPa, 46.5 MPa and 44.3 MPa for the SN5, SN10 and SN15 composites when compared with the untreated WAL/PLA composite. This shows that the effect of silane grafting improves the interfacial adhesion of WAL particle with the PLA matrix. It may improve the layer adhesion and exhibits higher flexural strength when compared with untreated composites (Vishal et al., 2023).

Fig. 6(b) shows the flexural modulus results of the untreated and silane treated WAL/PLA polymeric composite. The lowest flexural modulus of 590 MPa is detected on the neat 3D printed PLA composite. The addition of WAL particles in the PLA matrix shows an increasing trend in the flexural modulus value. Among the untreated composites, the composite with UN10 composition exploits the maximum flexural modulus value of 773 MPa compared with other untreated WAL/PLA composites. The reason for increased flexural modulus by the addition of WAL particles is that it reduces the brittleness of the composite. Likewise for the silane functionalized WAL/PLA polymeric composites, they show higher flexural modulus value of 689 MPa, 861 MPa and 758 MPa for the SN5, SN10 and SN15 composites. Among the observed results, the silane grafted 10% composition shows the highest flexural modulus value. The enhancement in flexural modulus can be attributed to the impact of silane grafting, which removes hemicellulose and other undesirable components, thereby increasing the stiffness of the composite. Silane grafting also has the potential to improve the interfacial adhesion with both the WAL particles and PLA matrix, resulting in a greater ability to transfer stress compared to untreated compositions. Similar results on the flexural modulus of the sugarcane bagasse fibre reinforced Poly Lactic Acid composite were reposted by Liu et al (Liu et al., 2019). In case of a higher concentration of WAL particle for both untreated and silane treated composites, it may reduce the flexural modulus, due to uneven load sharing in the interlayers of the composites.

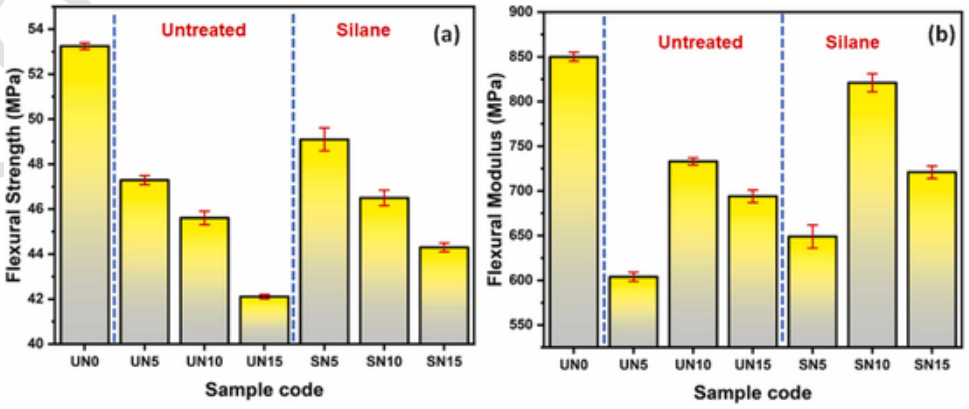

Fig. 6. (a) Flexural strength and (b) Flexural Modulus of WAL/PLA composites.

3.4.3. Compressive and Impact strength of WAL/PLA composites

Fig. 7(a) shows the compressive strength results of the untreated and silane treated WAL/PLA polymeric composite. A compressive strength value of 54.21 MPa, 63.40 MPa and 69.71 MPa is found for the 3D printed untreated WAL/PLA polymeric composites of UN5, UN10 and UN15 composites. Addition of WAL particle concentration has a positive impact on the compression property. The maximum compressive strength of 69.71 MPa is noticed on UN15 composites that is 43.75% higher than the neat 3D printed PLA composites. The reason for acquiring the higher compressive strength is due to uniform distribution of WAL particle in the PLA matrix. In case of silane grafted WAL particle reinforced composites, compressive strength of 59.51 MPa, 67.08 MPa and 74.32 MPa is read for the SN5, SN10 and SN15 composites. The silane treated WAL/PLA composites with same compositions which exhibits a higher compressive strength of 9.7%, 5% and 6.61% compared with the untreated WAL/PLA polymeric composites. The reason for the enhancement in the compressive properties is that, under compressive loading conditions the loading plane parallel along the printed layers, the uniformly distributed particle with better anchorage may fill the pores under the compressive load acting on the material (Zhu et al., 2017). This may improve the ultimate failure loading point than the untreated WAL particle reinforced composite.

Fig. 7(b) shows the impact strength results of the untreated and silane treated WAL particle reinforced PLA composite. The maximum impact strength of 9.8KJ/m² is observed for the silane grafted composite designated as SN10 composite. This is because of rapid transfer and high volume of energy absorption by the added WAL particles into the PLA polymeric matrix. Comparing the other untreated UN10 compositions with the silane treated SN10 designated composites shows an improved impact strength by 19.51%. It is due to a better interfacial adhesion obtained from the silane functional group attached on the WAL particles. Beyond 10% of silane treated WAL/PLA composite, the composite with UNI5 and SN15 exhibits 25.07% and 17.32% reduction in the impact strength value. The higher composition of the added WAL particles may hinder the layer adhesion and reduced the energy storage capacity of the composite. Similar result was reported for the graphene particle reinforced PEEK composites (Puértolas et al., 2019).

3.4.4. Melt flow index and D shore Hardness value of WAL/PLA composites

Fig. 8(a) shows the melt flow index value of the untreated and silane treated WAL/PLA polymeric composites. Melt flow index is used to measure the melting phenomenon of the polymeric filaments for 3D printing process. The result shows that, the melt flow index value decreases with an increase in the WAL particle composition. The maximum melt flow index value is detected for the neat PLA composition of 6.97 g/10 min. The lowest melt flow index value of 6.5 g/10 min is found for UN15 composites. This is an indication of the reduction in the polymeric viscosity and requires more load to extrude the filaments out from the nozzle. The reason for this decrease in the melt flow index value with respect to particle concentration is restriction of polymeric chain movement by the added WAL particle (Palaniyappan et al., 2023a). Compared to the silane treated WAL/PLA filaments the melt flow index value is higher about 4.3%, 5.9% and 15.3% for the 5%, 10% and 15% compositions. These results are a clear indication of the effect of silane treatment, the unwanted impurities present in the WAL particle surface are removed effectively and reduces the restriction of free molecular chain movement of the polymers. Palaniyappan et al. re-

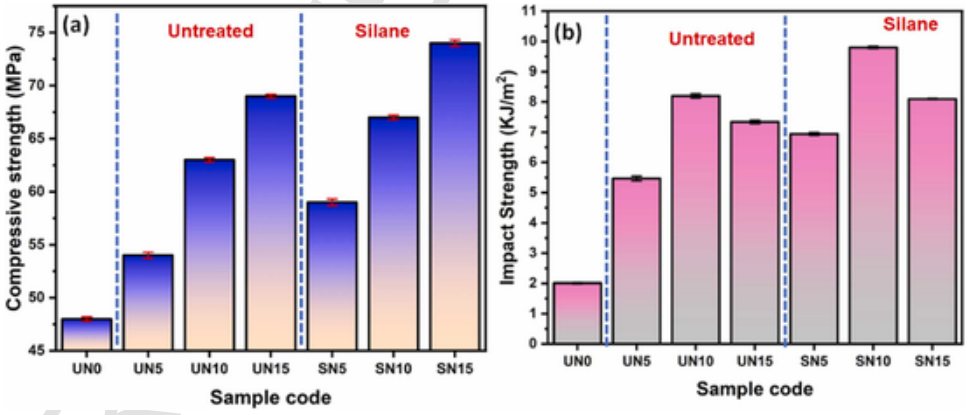

Fig. 7. (a) Compressive strength and (b) Impact strength results of WAL/PLA composites.

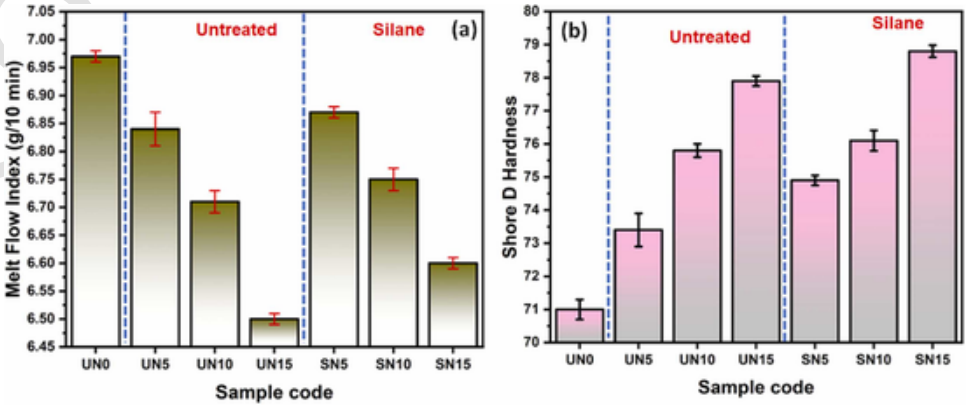

Fig. 8. (a) Melt flow index and (b) Shore hardness results of WAL/PLA composites.

ported similar outcomes on the extrusion of crab shell particle reinforced PLA composites (Palaniyappan et al., 2023b).

Fig. 8(b) shows the shore hardness results of the untreated and silane treated WAL/PLA polymeric composites. The shore hardness results for the untreated and silane treated WAL/PLA composites show that, the maximum hardness value for the untreated composites is 77.9% for UN15 composite and becomes 78.8% for SN 15 composite. The results of the neat 3D printed PLA composites exhibit the hardness value of 71 MPa, which is 10.98% and 9.71% lower for UN15 and SN 15 composites. Increase in the WAL particle concentration shows an improvement in the hardness value of the composite. This is due to added WAL particle which is harder and able to bear the applied load against indentation. The added particles are more rigid when compared to neat PLA polymer which may increase the rigidity and stiffness of the composite. By increasing the WAL particle concentration, the WAL particles are dispersed into the PLA polymeric matrix and occupies huge volume which bears more load against indentation (Palaniyappan et al., 2022). In the case of silane grafted WAL/PLA composites, the interfacial adhesion between each layer is enhanced, potentially making them better equipped to resist penetration by an indenter, in contrast to untreated WAL/PLA composites.

3.4.5. Heat deflection temperature and Contact angle of WAL/PLA 3D printed composites

Fig. 9(a) shows the heat deflection temperature results of the untreated and silane treated WAL/PLA polymeric composites. The measure of heat deflection temperature is used to analyses the softening working point of the respective composite, and this can be varied based on the type of reinforcements and fabrication route. The heat deflection temperature results of the neat PLA composite which is UN0 composition shows the lowest heat deflection temperature of 51 °C. The increase in the WAL particle concentration increases the heat deflection temperature for both the untreated and silane treated WAL/PLA polymeric composites. This is because of insulating characteristics of added WAL particles which increases the heat deflection temperature compared to neat PLA polymer.

The maximum heat deflection temperature of the untreated and silane treated WAL particle added composites is obtained for UN15 and SN15 composites as 62.21 °C and 63.79 °C. The improvement in the heat deflection temperature is that, the added WAL particles have better insulating characteristics when compared with the biodegradable PLA composites. In case of silane treated composites, the added silane functional group acts as a barrier on the WAL fillers to distribute the temperature faster. This may reduce the localized strain at a particular point and reduce the deflection rate with improved heat deflection temperature values (Huda et al., 2008).

Fig. 9(b) shows the contact angle results of the various compositions of untreated and silane treated WAL/PLA polymeric composite. The experimental contact angle results show that, the maximum contact angle value of 83.21° is detected for the neat 3D printed PLA specimens. It is an indication of hydrophobic behavior of PLA polymer which possesses lower wettability when associated with other WAL/PLA polymeric composites. An increase in the WAL particle concentration decreases the contact angle value, and the lowest contact angle value of 54.21° is observed on UN15 WAL/PLA polymeric composite. The introduction of WAL particles augments the presence of free hydroxyl groups within the PLA matrix. When these hydroxyl groups come into contact with water molecules, they readily absorb water, causing a decrease in the spherical shape of water droplets. This, in turn, can lead to a reduction in the contact angle for the respective composites and an increased tendency for the WAL/PLA composites to be hydrophilic. The untreated WAL/PLA composites of UN5, UN10, and UN15 observes lower contact angle value of 4%, 6.3% and 11.11% when compared with the silane treated WAL/PLA composites. The effect of silane grafting the silane layer acts as a barrier for the water molecule interaction and increases the hydrophobic tendency of the composite compared with the untreated WAL/PLA composite. Palaniyappan et al (Palaniyappan et al., 2023a). exploited similar results on the walnut shell added poly lactic acid. The addition of organic particles may decrease the contact angle drastically.

3.5. Water absorption behavior of WAL/PLA 3D printed composites

In this work, the 3D printed samples are exposed in three different kind of environmental conditions such as normal water, hot water and sea water. For the experimentation the deionized water is used for the normal and hot water conditions. In case of sea water condition, the water is collected from the Kovalam beach (India) and the pH is checked with pH meter. The measured pH values are in the range of 7.8–8.3 and used for the respective analysis. Fig. 10 shows the water absorption results for the various 3D printed WAL/PLA composites under different environmental conditions.

The water absorption phenomenon of various conditions such as normal, hot, and sea water condition is studied with respect to various WAL/PLA polymeric composites. The results show that, in all the conditions increasing in the WAL particle concentration in the PLA matrix increases the water absorption values. This is because of the combined action of both hydrophilic (WAL particles) and hydrophobic (PLA) behavior of the composite, and finally the composite behaves as an Amphipathic molecules type. From the radar distribution plot, both UN15 and SN15 composites exhibit higher water absorption value. In case of silane grafted composites, the water absorption is lower in order. This is owing to the effective removal of water absorbing molecules such as hemicellulose and lignin from the WAL particle. The rate of diffusivity is lower for the silane treated WAL/PLA polymeric composites compared with untreated WAL/PLA polymeric composites. Ramraji et al

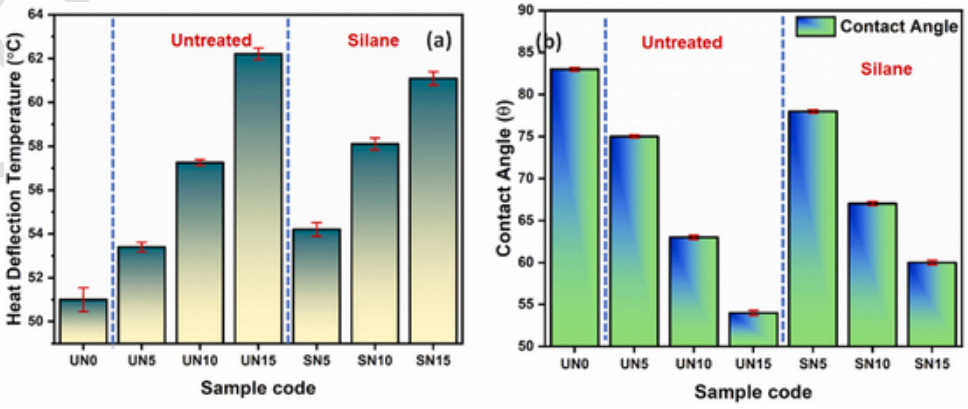

Fig. 9. (a) Heat deflection temperature and (b) Contact angle of WAL/PLA composites.

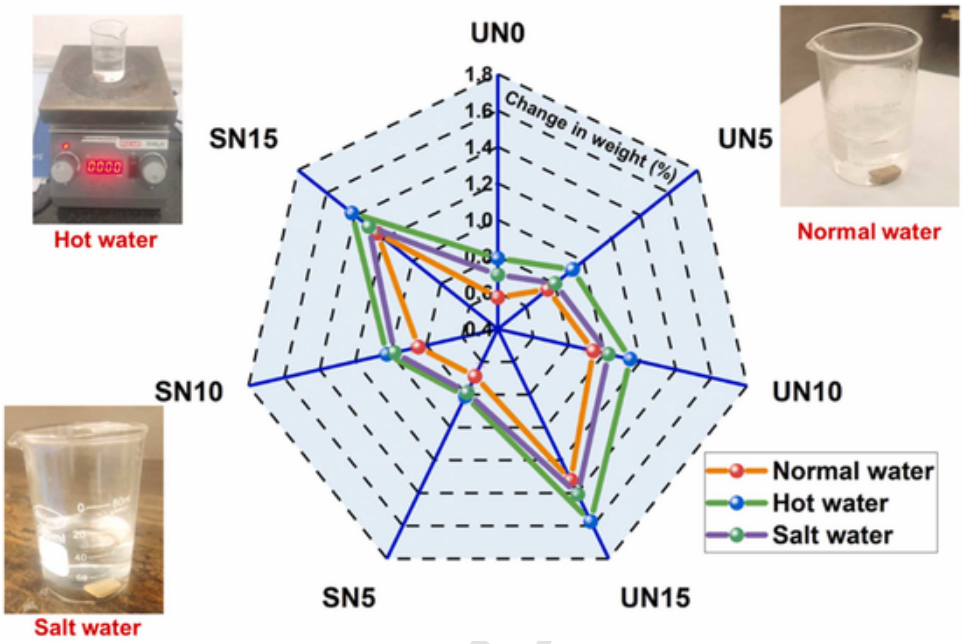

Fig. 10. Water absorption results of WAL/PLA composites under different conditions.

(Ramraji et al., 2019). observed similar results on the silane treated almond shell reinforced flax fibre epoxy composite. Silane treatment reduced the water absorption value than the untreated composite.

Among the various environmental conditions, the hot water conditions with UN15 composites show the maximum water absorption value of 1.573%. The reason for the increased diffusivity of water molecule is that composites 3D printed in multiple layers and the hot water may increase the rate of diffusivity of water molecule with the multiple pathways (layer gap and reinforcement porosity). It helps observing maximum water absorption value by the boosted diffusivity of hot water condition on UN15 and SN15 composites. For saltwater conditions, the water absorption values are higher than the normal water conditions samples. The maximum water absorption value of 1.408% and 1.304% is observed for UN15 and SN15 composites, and it is 6.5% and 4.9% lower than the normal water condition samples. The cause for the increased water uptake for the saltwater condition is that, the presence of sodium chloride in the water molecule may deposit on the composites, form an additional layer on the composite and uphold the water molecule inside the composites (Palaniyappan et al., 2022). The lowest water absorption from all the composites is observed for the SN5 composites as 0.688 under normal water condition. The sequential results for obtaining the lowest water absorption value for the WAL/PLA composites are normal water > salt water > hot water.

3.6. Bio degradation behavior of WAL/PLA 3D printed composites

Soil burial test of the prepared composite measures the biodegradation ability of the material under the natural environmental conditions. This result dictates the biodegradability of the composite. Fig. 11 shows the mass loss of the neat 3D printed PLA and WAL/PLA composite samples for the different time interval of 30- and 60-days. The lowest mass loss is observed on the neat PLA composites as 4.9% and 11.7% for the burial duration of 30 days and 60 days, respectively.

Increase in the WAL particle concentration in the polymer composites linearly increases the biodegradation ability of the composites. The maximum mass loss of 19.1% and 17.4% is obtained on the 3D printed WAL/PLA composite with UN15 and SN15 designated WAL/PLA composites. Maximum WAL particle loaded composites exhibits higher mass loss, and it is due to the added hydrophilic tendency WAL particle which readily observes water and has various open pockets for observing water. Therefore, the active places in the polar chain PLA polymer can interact readily with the microorganism. It may induce the kinetic growth rate of degradation of the polymeric materials. Similar observation on the biodegradation kinetics was reported by the Sekar et al. on the 3D printed wood particle reinforced PLA composite (Sekar et al., 2022).

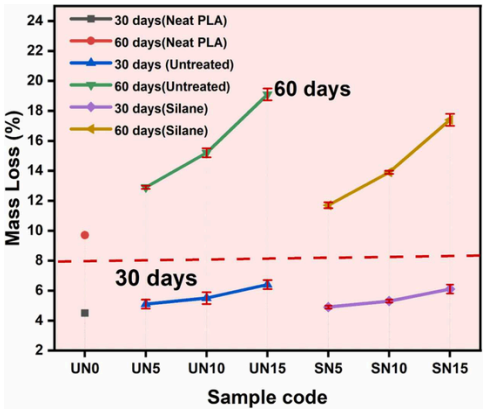

Fig. 11. Mass loss of the WAL/PLA composite under different durations.

Further considering various interval of mass loss of the samples, the soil buried WAL/PLA samples under 60 days of time interval shows higher mass loss. Considered UN15 and SN15 composites with 60 days of time interval samples exhibit of 7.54% and 6.49% higher mass loss when compared with the 30 days soil burial duration. This indicates that, higher burial time leads to steady state reaction of microorganism with the inner core of the WAL/PLA composites. The silane grafted composites of various compositions are compared with the untreated WAL/PLA and the neat PLA composites. The silane treated composite shows lesser mass loss compared with untreated WAL/PLA composite. The lowest mass loss value of 4.9% occurs on the UN5 composite with 30 days of soil burial duration. It is because the silane grafting may release the unwanted impurities such as microorganism, pectin, wax, and hemicellulose from the WAL particle surfaces. This may reduce the hydrophilicity of the particle that alters the free hydroxyl group that can interact easily with the microorganisms (Way et al., 2012). Therefore,

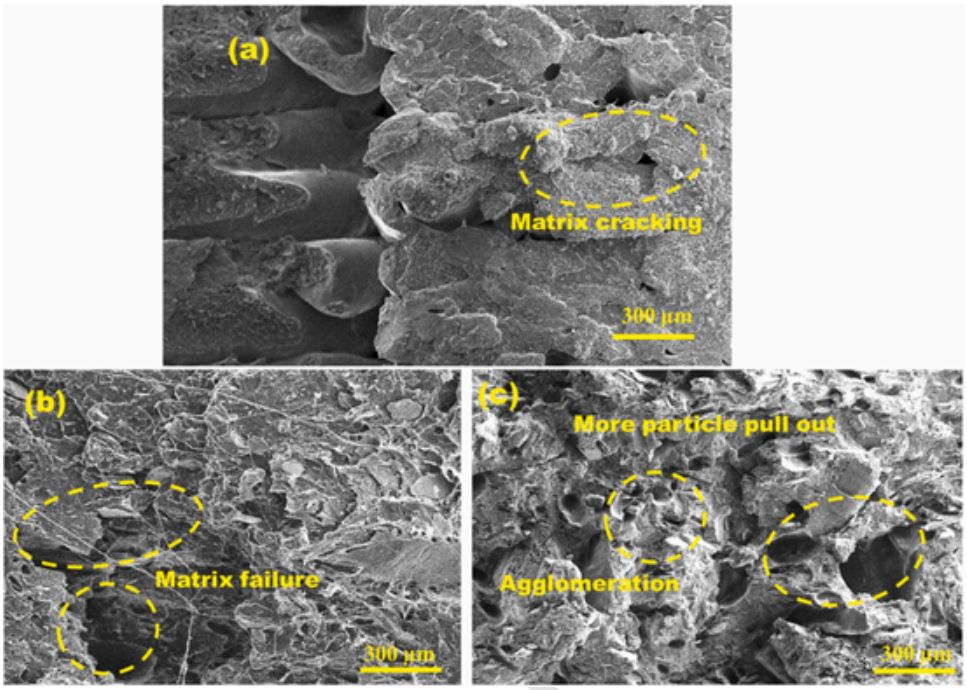

Fig. 12. SEM image of untreated WAL/PLA composites, (a)UNO, (b) UN5, and (c), UN15.

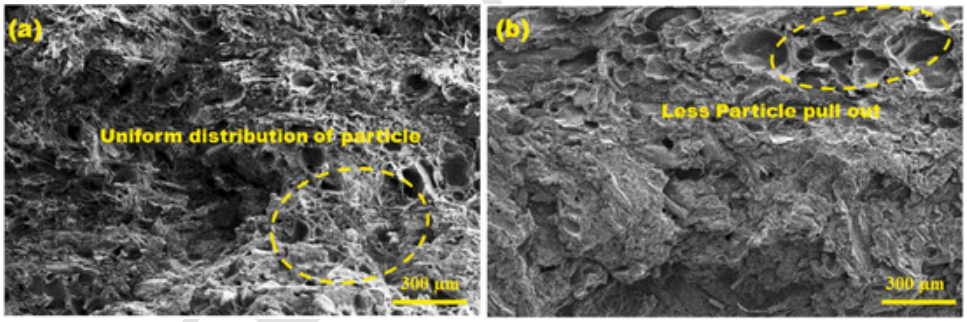

Fig. 13. SEM image of silane treated WAL/PLA composites (a) SN10, and (b) SN15.

this may take time for the degradation kinetics of the silane treated WAL/PLA composites.

3.7. Fractographical studies of the neat PLA and WAL/PLA composites

Fig. 12 shows the tensile fractography of the 3D printed neat PLA and WAL/PLA composites. Fig. 12 (a) shows the fractured tensile samples of neat PLA composites. The results show that the printing layers with the presence of cleavage mode of fracture which is an indication of brittle mode of failure of the samples. In case of UN5 composites fractured macroscopic image of Fig. 12 (b), the matrix cracking is a predominant mode of fracture which is a hint of the added WAL particles not enough to transfer the stress to the polymeric matrix. Considering UN15 composites, the fractographical image in Fig. 12 (c) clearly shows the presence of a greater number of particle pull-outs. Physically bonded added WAL particle does not withstand the higher load and starts to pultrude from the matrix surfaces under tensile loading, and it may end up in severe particle pull out on the fractured surface. Similar experimental observation on the 3D printed almond shell reinforced PLA composite was reported, the experimental results show that at higher concentration of almond shell particles, more particles pull out were also observed (Singh et al., 2020b).

Fig. 13 shows the tensile fractography of the silane treated WAL/PLA composites. For silane treated condition of SN10 samples, the particles were evenly dispersed in the polymeric matrix which is depicted in Fig. 13 (a). There is an absence of matrix cracking which clearly shows that the applied load is evenly shared in the polymeric matrix. Considering SN15 composites in Fig. 13 (b), at higher particle loading there is a minimum number of particle pull-outs when compared with UN15 composites. This is because the silane chemical grafting may improve the interfacial adhesion that results in lesser delamination occurred on the SN15 composites. Similar observation on the silane treated cork particle reinforced acrylonitrile – styrene – butyl acrylate composite was reported (de León et al., 2022).

3.8. Application of the developed composite filaments

From the raw materials to the end products, the energy spent for bio-composite development is lower when utilizing 3D printing technology and inorganic reinforcement. Nowadays, various end products are required for human things. Various end products are designed and 3D printed using a design file based on individual needs. In the current study, the developed bio-composites of SN10 composite filaments are used for the 3D printing process to create an oval food serving basket. Fig. 14 shows the design file and printing procedure of the developed WAL/PLA bio-composite. Based on the heat deflection temperature results, the material can withstand higher temperatures when compared with neat PLA composite. This sustainable bio-composite with organic

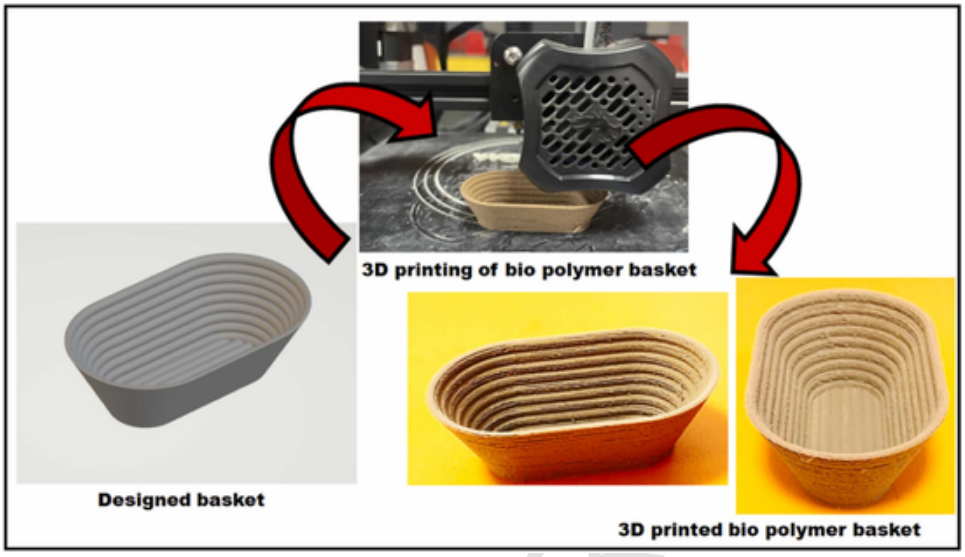

Fig. 14. Application of the WAL/PLA composite for food packaging industries.

reinforcements and 3D printability can be a potential material for the food packaging industry; after end use, the materials can degrade faster than conventional polymers. From the aesthetic appearance of this bio-composite, this added wood particle may appear similar to the wood colour and attract the customer's attention.

4. Conclusion

Silane grafted WAL particles with different fractions was used to improve the mechanical, thermal and biodegradation property of the 3D printed polylactic acid bio-composite. Silane grafting improves the organic particle interfacial adhesion and mechanical properties such as tensile, flexural, compression and impact strength compared with the untreated 3D printed composites.

- The addition of WAL particle decreases the tensile and flexural strength, but in case of modulus, the values are improved when compared with neat Poly lactic acid composites.
- The maximum heat deflection temperature of the untreated and silane treated particle added to WAL/PLA composites is obtained for UN15 and SN15 composites as 62.21° and 63.79°.
- The maximum mass loss of 19.1% and 17.4% is obtained for the 3D printed WAL/PLA composite with UN15 and SN15 designated composites.
- The sequential results for obtaining the lowest water absorption value for the WAL/PLA composites are normal water > salt water > hot water.

The combined results of better mechanical performance and better biodegradation property of the 3D printed WAL/PLA composite prove the high potential of the bio-composite as a sustainable material for the food packaging industries. The developed bio-composites promote sustainability in a new era of circular economy by offering an eco-friendly solution that aligns with the principles of waste reduction, resource efficiency, and a closed-loop system for a more environmentally conscious future.

CRediT authorship contribution statement

Sabarinathan Palaniyappan: Conceptualization, Investigation, Writing – review & editing. Supervision. **Narain kumar Sivakumar**: Experimentation, Writing Validation. **Mahdi Bodaghi:** Writing validation, Writing – review & editing, Supervision. **Mostafizur Rahaman:** Resources, Funding acquisition, Writing Validation. **Saravanan Pandiaraj:** Resources, Funding acquisition, Writing Validation.

Declaration of Competing Interest

The authors declare that they have no known competing financial interests or personal relationships that could have appeared to influence the work reported in this paper.

Data Availability

No data was used for the research described in the article.

Acknowledgment

The authors acknowledge the Researchers Supporting Project number (RSPD2023R674), King Saud University, Riyadh, Saudi Arabia for funding this research work.

References

Ahmed, J., Santhosh, R., Thakur, R., Mulla, M., & Sarkar, P. (2023). *Thermo-mechanical, rheological, microstructural, and barrier properties of gum-based edible packaging: A review. Food Packaging and Shelf Life*, *38*, 101117.

Dang, Z.M., Yuan, J.K., Zha, J.W., Zhou, T., Li, S.T., & Hu, G.H. (2012). *Fundamentals, processes and applications of high-permittivity polymer–matrix composites. Progress in Materials Science*, *57*(4), 660–723.

Vroman, I., & Tighzert, L. (2009). *Biodegradable polymers. Materials*, *2*(2), 307–344.

Song, J.H., Murphy, R.J., Narayan, R., & Davies, G.B.H. (2009). *Biodegradable and compostable alternatives to conventional plastics. Philosophical Transactions of the Royal Society B: Biological Sciences*, *364*(1526), 2127–2139.

Silveira, V.A.I., Marim, B.M., Hipólito, A., Gonçalves, M.C., Mali, S., Kobayashi, R.K.T., & Celligoi, M.A.P.C. (2020). *Characterization and antimicrobial properties of bioactive packaging films based on polylactic acid-sophorolipid for the control of foodborne pathogens. Food Packaging and Shelf Life*, *26*, 100591.

Rasal, R.M., Janorkar, A.V., & Hirt, D.E. (2010). *Poly(lactic acid) modifications. Progress in Polymer Science*, *35*, 338–356.

Li, X., Qiu, C., Ji, N., Sun, C., Xiong, L., & Sun, Q. (2015). *Mechanical, barrier and morphological properties of starch nanocrystals-reinforced pea starch films. Carbohydrate Polymers*, *121*, 155–162.

Du, Y., Wu, T., Yan, N., Kortschot, M.T., & Farnood, R. (2014). *Fabrication and characterization of fully biodegradable natural fiber-reinforced poly (lactic acid) composites. Composites Part B: Engineering*, *56*, 717–723.

Zhang, R., Lan, W., Ji, T., Sameen, D.E., Ahmed, S., Qin, W., & Liu, Y. (2021). *Development of polylactic acid/ZnO composite membranes prepared by ultrasonication and electrospinning for food packaging. Lwt*, *135*, 110072.

Palaniyappan, S., Veiravan, A., Kaliyamoorthy, R., Kumar, V., & Veeman, D. (2022). *A spatial distribution effect of almond shell bio filler on physical, mechanical, thermal*

deflection and water absorption properties of vinyl ester polymer composite. Polymer Composites, 43(5), 3204–3218.
Essabir, H., Hilali, E., Elgharad, A., El Minor, H., Imad, A., Elamraoui, A., & Al Gaoudi, O. (2013). *Mechanical and thermal properties of bio-composites based on polypropylene reinforced with Nut-shells of Argan particles. Materials & Design, 49*, 442–448.
Cheang, P., & Khor, K.A. (2003). *Effect of particulate morphology on the tensile behaviour of polymer–hydroxyapatite composites. Materials Science and Engineering: A, 345*(1–2), 47–54.
John, M.J., & Thomas, S. (2008). *Biofibres and biocomposites. Carbohydrate Polymers, 71*(3), 343–364.
Hemmati, F., Jafari, S.M., Kashaninejad, M., & Motlagh, M.B. (2018). *Synthesis and characterization of cellulose nanocrystals derived from walnut shell agricultural residues. International Journal of Biological macromolecules, 120*, 1216–1224.
Demiral, İ., & Kul, Ş.Ç. (2014). *Pyrolysis of apricot kernel shell in a fixed-bed reactor: Characterization of bio-oil and char. Journal of Analytical and Applied Pyrolysis, 107*, 17–24.
Pirayesh, H., Khazaeian, A., & Tabarsa, T. (2012). *The potential for using walnut (Juglans regia L.) shell as a raw material for wood-based particleboard manufacturing. Composites Part B: Engineering, 43*(8), 3276–3280.
Ayrilmis, N., Kariz, M., Kwon, J.H., & Kitek Kuzman, M. (2019). *Effect of printing layer thickness on water absorption and mechanical properties of 3D-printed wood/PLA composite materials. The International Journal of Advanced Manufacturing Technology, 102*, 2195–2200.
Sarsari, N.A., Pourmousa, S., & Tajdini, A. (2016). *Physical and mechanical properties of walnut shell flour-filled thermoplastic starch composites. Bioresources, 11*(3), 6968–6983.
Liu, J., Yang, X., Liu, Y., Wei, Z., & Zhang, X. (2014). *Effect of surface modification of walnut shell on properties of poly (lactic acid)/walnut shell powder composites. China Plast, 28*(3), 40–45.
Vishal, K., Rajkumar, K., Nitin, M.S., & Sabarinathan, P. (2022). *Kigelia africana fruit biofibre polysaccharide extraction and biofibre development by silane chemical treatment. International Journal of Biological Macromolecules, 209*, 1248–1259.
Tran, T.P.T., Bénézet, J.C., & Bergeret, A. (2014). *Rice and Einkorn wheat husks reinforced poly (lactic acid)(PLA) biocomposites: Effects of alkaline and silane surface treatments of husks. Industrial Crops and Products, 58*, 111–124.
Zhou, M., Wan, G., Wang, G., Wieme, T., Edeleva, M., Cardon, L., & D'hooge, D.R. (2023). *Carbon Nitride Grafting Modification of Poly (lactic acid) to Maximize UV Protection and Mechanical Properties for Packaging Applications. ACS Applied Materials & Interfaces*.
Sun, Y., Zhang, Z., Wang, Y., Wang, J., Zheng, Z., Yang, B., & Xu, G. (2023). *Effect of silane coupling agent on the ultraviolet weathering behavior of polylactic acid-based composites. International Journal of Polymer Analysis and Characterization, 28*(5), 509–522.
Mathiazhagan, N., Sivakumar, N.K., Palaniyappan, S., & Rahaman, M. (2023). *Influence of printing-based factors on the mechanical properties of hexagonal lattice-structured 3D printed novel walnut shell/polylactic acid composite. Journal of Thermoplastic Composite Materials*. 08927057231185711.
Peterson, A.M. (2019). *Review of acrylonitrile butadiene styrene in fused filament fabrication: A plastics engineering-focused perspective. Additive Manufacturing, 27*, 363–371.
Veeman, D., & Palaniyappan, S. (2022). *Process optimisation on the compressive strength property for the 3D printing of PLA/almond shell composite. Journal of Thermoplastic Composite Materials*. 08927057221092327.
Singh, R., Kumar, R., Singh, M., & Preet, P. (2020a). *On compressive and morphological features of 3D printed almond skin powder reinforced PLA matrix. Materials Research Express, 7*(2), 025311.
Yurttas, E., Tetik, N., & Ayrilmis, N. (2023). *Antimicrobial properties of 3D printed biocomposites with heat-treated wood flour using silver nanoparticles with leaf extract. Wood Material Science & Engineering, 18*(2), 663–671.
Ahmed, J., Mulla, M.Z., Vahora, A., Bher, A., & Auras, R. (2021). *Morphological, barrier and thermo-mechanical properties of high-pressure treated polylactide graphene oxide reinforced composite films. Food Packaging and Shelf Life, 29*, 100702.
Yurttas, E., & Ayrilmis, N. (2023). *Mechanical and Thermal Properties of 3D-Printed Biocomposites of Polylactic Acid and Thermally Modified Wood Flour with Silver Nanoparticles. Macromolecular Materials and Engineering*, 2300180.
Sawpan, M.A., Pickering, K.L., & Fernyhough, A. (2011). *Effect of various chemical treatments on the fibre structure and tensile properties of industrial hemp fibres. Composites Part A: Applied Science and Manufacturing, 42*(8), 888–895.
Hong, C.K., Hwang, I., Kim, N., Park, D.H., Hwang, B.S., & Nah, C. (2008). *Mechanical properties of silanized jute–polypropylene composites. Journal of Industrial and Engineering Chemistry, 14*(1), 71–76.
Manimaran, P., Pillai, G.P., Vignesh, V., & Prithiviraj, M. (2020). *Characterization of natural cellulosic fibers from Nendran Banana Peduncle plants. International Journal of Biological Macromolecules, 162*, 1807–1815.
Sabarinathan, P., Rajkumar, K., Annamalai, V.E., & Vishal, K. (2020). *Characterization on chemical and mechanical properties of silane treated fish tail palm fibres. International Journal of Biological Macromolecules, 163*, 2457–2464.
Cai, M., Takagi, H., Nakagaito, A.N., Katoh, M., Ueki, T., Waterhouse, G.I., & Li, Y. (2015). *Influence of alkali treatment on internal microstructure and tensile properties of abaca fibers. Industrial Crops and Products, 65*, 27–35.
Sreekumar, P.A., Saiah, R., Saiter, J.M., Leblanc, N., Joseph, K., Unnikrishnan, G., & Thomas, S. (2009). *Dynamic mechanical properties of sisal fiber reinforced polyester composites fabricated by resin transfer molding. Polymer Composites, 30*(6), 768–775.
Phuong, L.X., Shida, S., & Saito, Y. (2007). *Effects of heat treatment on brittleness of Styrax tonkinensis wood. Journal of Wood Science, 53*(3), 181–186.
Luo, H., Zhang, C., Xiong, G., & Wan, Y. (2016). *Effects of alkali and alkali/silane treatments of corn fibers on mechanical and thermal properties of its composites with polylactic acid. Polymer Composites, 37*(12), 3499–3507.
Liu, R., Luo, S., Cao, J., & Chen, Y. (2016). *Mechanical properties of wood flour/poly (lactic acid) composites coupled with waterborne silane-polyacrylate copolymer emulsion. Holzforschung, 70*(5), 439–447.
Hamming, L.M., Qiao, R., Messersmith, P.B., & Brinson, L.C. (2009). *Effects of dispersion and interfacial modification on the macroscale properties of TiO2 polymer–matrix nanocomposites. Composites Science and Technology, 69*(11–12), 1880–1886.
Liu, H., He, H., Peng, X., Huang, B., & Li, J. (2019). *Three-dimensional printing of poly (lactic acid) bio-based composites with sugarcane bagasse fiber: Effect of printing orientation on tensile performance. Polymers for Advanced Technologies, 30*(4), 910–922.
Vishal, K., Rajkumar, K., Sabarinathan, P., & Arun, A. (2023). *Mechanical and thermal characteristics of steam-exploded silane grafted Kigelia Pinnata fruit (KPF) fiber reinforced vinyl ester polymer composites. Polym Compos, 1*, 1.
Zhu, J., Hu, Y., Tang, Y., & Wang, B. (2017). *Effects of styrene–acrylonitrile contents on the properties of ABS/SAN blends for fused deposition modeling. Journal of Applied Polymer Science, 134*(7).
Puértolas, J.A., Castro, M., Morris, J.A., Ríos, R., & Ansón-Casaos, A. (2019). *Tribological and mechanical properties of graphene nanoplatelet/PEEK composites. Carbon, 141*, 107–122.
Palaniyappan, S., Annamalai, G., Kumar Sivakumar, N., & Muthu, P. (2023a). *Development of functional gradient multi-material composites using Poly Lactic Acid and walnut shell reinforced Poly Lactic Acid filaments by fused filament fabrication technology. Journal of Building Engineering, 65*, 105746.
Palaniyappan, S., Sivakumar, N.K., & Sekar, V. (2023b). *Sustainable approach to the revalorization of crab shell waste in polymeric filament extrusion for 3D printing applications. Biomass Conversion and Biorefinery*, 1–18.
Huda, M.S., Drzal, L.T., Mohanty, A.K., & Misra, M. (2008). *Effect of fiber surface-treatments on the properties of laminated biocomposites from poly (lactic acid)(PLA) and kenaf fibers. Composites Science and Technology, 68*(2), 424–432.
Ramraji, K., Rajkumar, K., & Sabarinathan, P. (2019). *Tailoring of tensile and dynamic thermomechanical properties of interleaved chemical-treated fine almond shell particulate flax fiber stacked vinyl ester polymeric composites. Proceedings of the Institution of Mechanical Engineers, Part L: Journal of Materials: Design and Applications, 233*(11), 2311–2322.
Sekar, V., Eh Noum, S.Y., Sivanesan, S., Putra, A., Chin Vui Sheng, D.D., & Kassim, D.H. (2022). *Effect of thickness and infill density on acoustic performance of 3D printed panels made of natural fiber reinforced composites. Journal of Natural Fibers, 19*(13), 7132–7140.
Way, C., Dean, K., Wu, D.Y., & Palombo, E. (2012). *Biodegradation of sequentially surface treated lignocellulose reinforced polylactic acid composites: Carbon dioxide evolution and morphology. Polymer Degradation and Stability, 97*(3), 430–438.
Singh, R., Kumar, R., Singh, M., & Preet, P. (2020b). *On compressive and morphological features of 3D printed almond skin powder reinforced PLA matrix. Materials Research Express, 7*(2), 025311.
de León, A.S., Núñez-Gálvez, F., Moreno-Sánchez, D., Fernández-Delgado, N., & Molina, S.I. (2022). *Polymer composites with cork particles functionalized by surface polymerization for fused deposition modeling. ACS Applied Polymer Materials, 4*(2), 1225–1233.